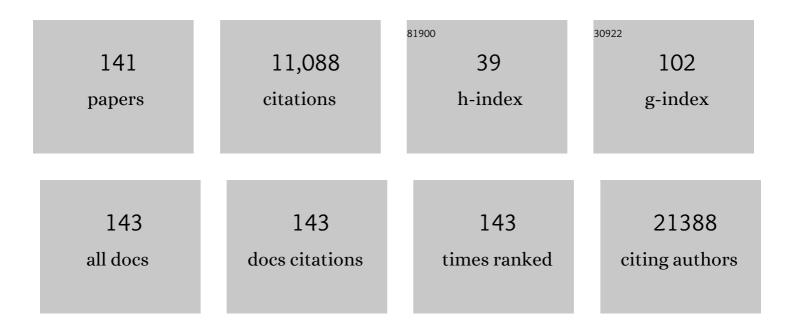
List of Publications by Year in descending order

Source: https://exaly.com/author-pdf/327441/publications.pdf Version: 2024-02-01



#	Article	IF	CITATIONS
1	LC3B is an RNA-binding protein to trigger rapid mRNA degradation during autophagy. Nature Communications, 2022, 13, 1436.	12.8	39
2	Mitochondrial protease ClpP supplementation ameliorates diet-induced NASH in mice. Journal of Hepatology, 2022, 77, 735-747.	3.7	8
3	LAG-3xPD-L1 bispecific antibody potentiates antitumor responses of TÂcells through dendritic cell activation. Molecular Therapy, 2022, 30, 2800-2816.	8.2	29
4	Structural insights into ClpP protease side exit poreâ€opening by a pH drop coupled with substrate hydrolysis. EMBO Journal, 2022, 41, e109755.	7.8	8
5	TRAF6-mediated ubiquitination of MST1/STK4 attenuates the TLR4-NF-κB signaling pathway in macrophages. Cellular and Molecular Life Sciences, 2021, 78, 2315-2328.	5.4	10
6	Tyrosyltyrosylcysteine-Directed Synthesis of Chiral Cobalt Oxide Nanoparticles and Peptide Conformation Analysis. ACS Nano, 2021, 15, 979-988.	14.6	19
7	UXT chaperone prevents proteotoxicity by acting as an autophagy adaptor for p62-dependent aggrephagy. Nature Communications, 2021, 12, 1955.	12.8	9
8	Phospholipid transfer function of PTPIP51 at mitochondriaâ€essociated ER membranes. EMBO Reports, 2021, 22, e51323.	4.5	54
9	Translation mediated by the nuclear cap-binding complex is confined to the perinuclear region via a CTIF–DDX19B interaction. Nucleic Acids Research, 2021, 49, 8261-8276.	14.5	10
10	Dynamics and Entropy of Cyclohexane Rings Control pH-Responsive Reactivity. Jacs Au, 2021, 1, 2070-2079.	7.9	3
11	Structural basis for the Nâ€degron specificity of <scp>ClpS1</scp> from <scp><i>Arabidopsis thaliana</i></scp> . Protein Science, 2021, 30, 700-708.	7.6	15
12	Aminopeptidases trim Xaa-Pro proteins, initiating their degradation by the Pro/N-degron pathway. Proceedings of the National Academy of Sciences of the United States of America, 2021, 118, .	7.1	13
13	Crystal structure of yeast Gid10 in complex with Pro/N-degron. Biochemical and Biophysical Research Communications, 2021, 582, 86-92.	2.1	9
14	Use of the LC3B-fusion technique for biochemical and structural studies of proteins involved in the N-degron pathway. Journal of Biological Chemistry, 2020, 295, 2590-2600.	3.4	14
15	Metabolic engineering of Escherichia coli to produce a monophosphoryl lipid A adjuvant. Metabolic Engineering, 2020, 57, 193-202.	7.0	16
16	Enhancing Protein Crystallization under a Magnetic Field. Crystals, 2020, 10, 821.	2.2	9
17	Targeted Degradation of Transcription Coactivator SRCâ€l through the Nâ€Degron Pathway. Angewandte Chemie, 2020, 132, 17701-17708.	2.0	2
18	Targeted Degradation of Transcription Coactivator SRCâ€1 through the Nâ€Degron Pathway. Angewandte Chemie - International Edition, 2020, 59, 17548-17555.	13.8	22

#	Article	IF	CITATIONS
19	A host dTMP-bound structure of T4 phage dCMP hydroxymethylase mutant using an X-ray free electron laser. Scientific Reports, 2019, 9, 16316.	3.3	2
20	Structural and Mechanistic Insights into Caffeine Degradation by the Bacterial N-Demethylase Complex. Journal of Molecular Biology, 2019, 431, 3647-3661.	4.2	26
21	Endoribonucleolytic Cleavage of m6A-Containing RNAs by RNase P/MRP Complex. Molecular Cell, 2019, 74, 494-507.e8.	9.7	371
22	MST1 Negatively Regulates TNFα-Induced NF-κB Signaling through Modulating LUBAC Activity. Molecular Cell, 2019, 73, 1138-1149.e6.	9.7	39
23	elF4A3 Phosphorylation by CDKs Affects NMD during the Cell Cycle. Cell Reports, 2019, 26, 2126-2139.e9.	6.4	36
24	pH-dependent regulation of SQSTM1/p62 during autophagy. Autophagy, 2019, 15, 180-181.	9.1	12
25	A cytosine modification mechanism revealed by the structure of a ternary complex of deoxycytidylate hydroxymethylase from bacteriophage T4 with its cofactor and substrate. IUCrJ, 2019, 6, 206-217.	2.2	4
26	Structural studies of a novel ubiquitin-modifying enzyme, SdeA, using various tools. Acta Crystallographica Section A: Foundations and Advances, 2019, 75, a78-a78.	0.1	0
27	Unveiling the pathway to Z-DNA in the protein-induced B–Z transition. Nucleic Acids Research, 2018, 46, 4129-4137.	14.5	36
28	Structural and Biochemical Study of the Mono-ADP-Ribosyltransferase Domain of SdeA, a Ubiquitylating/Deubiquitylating Enzyme from Legionella pneumophila. Journal of Molecular Biology, 2018, 430, 2843-2856.	4.2	24
29	Insights into degradation mechanism of N-end rule substrates by p62/SQSTM1 autophagy adapter. Nature Communications, 2018, 9, 3291.	12.8	62
30	The C-terminal region of ATG101 bridges ULK1 and PtdIns3K complex in autophagy initiation. Autophagy, 2018, 14, 2104-2116.	9.1	40
31	PELI1 Selectively Targets Kinase-Active RIP3 for Ubiquitylation-Dependent Proteasomal Degradation. Molecular Cell, 2018, 70, 920-935.e7.	9.7	77
32	A Structural View of Xenophagy, a Battle between Host and Microbes. Molecules and Cells, 2018, 41, 27-34.	2.6	34
33	Structural insight into degradation mechanism of N-end rule substrates by p62/SQSTM1 selective autophagy adaptor. Acta Crystallographica Section A: Foundations and Advances, 2018, 74, a313-a313.	0.1	0
34	ACCORD: an assessment tool to determine the orientation of homodimeric coiled-coils. Scientific Reports, 2017, 7, 43318.	3.3	6
35	Structural Characterization of <scp>RNA</scp> Recognition Motifâ€2 Domain of <scp>SART3</scp> . Bulletin of the Korean Chemical Society, 2017, 38, 444-447.	1.9	1
36	A novel conformation of the LC3-interacting region motif revealed by the structure of a complex between LC3B and RavZ. Biochemical and Biophysical Research Communications, 2017, 490, 1093-1099.	2.1	26

#	Article	IF	CITATIONS
37	The 1:2 complex between RavZ and LC3 reveals a mechanism for deconjugation of LC3 on the phagophore membrane. Autophagy, 2017, 13, 70-81.	9.1	37
38	An assessment tool for determination of coiled-coil orientation. Acta Crystallographica Section A: Foundations and Advances, 2017, 73, a118-a118.	0.1	0
39	Structural Studies of Peptide Binding Interaction of HCV IRES Domain IV. Journal of the Korean Magnetic Resonance Society, 2017, 21, 109-113.	0.1	0
40	Structure biology of selective autophagy receptors. BMB Reports, 2016, 49, 73-80.	2.4	54
41	A facile method to prepare large quantities of active caspase-3 overexpressed by auto-induction in the C41(DE3) strain. Protein Expression and Purification, 2016, 126, 104-108.	1.3	7
42	The structure of the pleiotropic transcription regulator CodY provides insight into its GTP-sensing mechanism. Nucleic Acids Research, 2016, 44, gkw775.	14.5	18
43	Structural basis for dual specificity of yeast N-terminal amidase in the N-end rule pathway. Proceedings of the National Academy of Sciences of the United States of America, 2016, 113, 12438-12443.	7.1	22
44	Guidelines for the use and interpretation of assays for monitoring autophagy (3rd edition). Autophagy, 2016, 12, 1-222.	9.1	4,701
45	Structural Characterization of pre-miRNA 155. Journal of the Korean Magnetic Resonance Society, 2016, 20, 46-49.	0.1	0
46	A key lysine residue in the AXH domain of ataxin-1 is essential for its ubiquitylation. Biochimica Et Biophysica Acta - Proteins and Proteomics, 2015, 1854, 356-364.	2.3	14
47	mTRAQ-based quantitative analysis combined with peptide fractionation based on cysteinyl peptide enrichment. Analytical Biochemistry, 2015, 477, 41-49.	2.4	3
48	PEAâ€15 facilitates EGFR dephosphorylation <i>via</i> ERK sequestration at increased ER–PM contacts in TNBC cells. FEBS Letters, 2015, 589, 1033-1039.	2.8	11
49	Mitochondrial ATP synthase activity is impaired by suppressed <i>O</i> -GlcNAcylation in Alzheimer's disease. Human Molecular Genetics, 2015, 24, 6492-6504.	2.9	74
50	Insights into autophagosome maturation revealed by the structures of ATG5 with its interacting partners. Autophagy, 2015, 11, 75-87.	9.1	59
51	Swapping of interaction partners with ATG5 for autophagosome maturation. BMB Reports, 2015, 48, 129-130.	2.4	9
52	Insulin activates EGFR by stimulating its interaction with IGF-1R in low-EGFR-expressing TNBC cells. BMB Reports, 2015, 48, 342-347.	2.4	9
53	Direct recognition of the C-terminal polylysine residues of nonstop protein by Ltn1, an E3 ubiquitin ligase. Biochemical and Biophysical Research Communications, 2014, 453, 642-647.	2.1	2
54	Crystallization and preliminary X-ray analysis of the C-terminal fragment of Ski7 fromSaccharomyces cerevisiae. Acta Crystallographica Section F, Structural Biology Communications, 2014, 70, 1252-1255.	0.8	1

#	Article	IF	CITATIONS
55	Expansion of the clinicopathological and mutational spectrum of Perry syndrome. Parkinsonism and Related Disorders, 2014, 20, 388-393.	2.2	24
56	elF4AIII enhances translation of nuclear cap-binding complex–bound mRNAs by promoting disruption of secondary structures in 5â€2UTR. Proceedings of the National Academy of Sciences of the United States of America, 2014, 111, E4577-86.	7.1	62
57	Insights into the Molecular Evolution of HslU ATPase through Biochemical and Mutational Analyses. PLoS ONE, 2014, 9, e103027.	2.5	2
58	Structural basis for recognition of autophagic receptor NDP52 by the sugar receptor galectin-8. Nature Communications, 2013, 4, 1613.	12.8	91
59	Differential in vitro and cellular effects of iron chelators for hypoxia inducible factor hydroxylases. Journal of Cellular Biochemistry, 2013, 114, 864-873.	2.6	29
60	MG53-induced IRS-1 ubiquitination negatively regulates skeletal myogenesis and insulin signalling. Nature Communications, 2013, 4, 2354.	12.8	140
61	InÂvivo fluorescence imaging for cancer diagnosis using receptor-targeted epidermal growth factor-based nanoprobe. Biomaterials, 2013, 34, 9149-9159.	11.4	33
62	Crystal structure of the single cystathionine β-synthase domain-containing protein CBSX1 from Arabidopsis thaliana. Biochemical and Biophysical Research Communications, 2013, 430, 265-271.	2.1	5
63	Change in single cystathionine \hat{l}^2 -synthase domain-containing protein from a bent to flat conformation upon adenosine monophosphate binding. Journal of Structural Biology, 2013, 183, 40-46.	2.8	14
64	Renal Protective Effects of Toll-like Receptor 4 Signaling Blockade in Type 2 Diabetic Mice. Endocrinology, 2013, 154, 2144-2155.	2.8	79
65	Rapid degradation of replication-dependent histone mRNAs largely occurs on mRNAs bound by nuclear cap-binding proteins 80 and 20. Nucleic Acids Research, 2013, 41, 1307-1318.	14.5	29
66	Structural and Biochemical Analyses of the Eukaryotic Heat Shock Locus V (HslV) from Trypanosoma brucei. Journal of Biological Chemistry, 2013, 288, 23234-23243.	3.4	8
67	Structure of the autophagic E2 enzyme Atg10. Acta Crystallographica Section D: Biological Crystallography, 2012, 68, 1409-1417.	2.5	26
68	Structures of the ribosome-inactivating protein from barley seeds reveal a unique activation mechanism. Acta Crystallographica Section D: Biological Crystallography, 2012, 68, 1488-1500.	2.5	8
69	Backbone resonances assignment of 19ÂkDa CD1 domain of human mitotic checkpoint serine/threonine-protein kinase, Bub1. Biomolecular NMR Assignments, 2012, 6, 109-113.	0.8	3
70	Crystal structure of <i>Pyrococcus furiosus</i> PF2050, a member of the DUF2666 protein family. FEBS Letters, 2012, 586, 1384-1388.	2.8	0
71	Insights into noncanonical E1 enzyme activation from the structure of autophagic E1 Atg7 with Atg8. Nature Structural and Molecular Biology, 2011, 18, 1323-1330.	8.2	89
72	Crystal structure of ubiquitin-like small archaeal modifier protein 1 (SAMP1) from Haloferax volcanii. Biochemical and Biophysical Research Communications, 2011, 405, 112-117.	2.1	22

#	Article	IF	CITATIONS
73	Crystal Structure of a Coiled-Coil Domain from Human ROCK I. PLoS ONE, 2011, 6, e18080.	2.5	31
74	Ubiquitin Ligases of the N-End Rule Pathway: Assessment of Mutations in UBR1 That Cause the Johanson-Blizzard Syndrome. PLoS ONE, 2011, 6, e24925.	2.5	40
75	Structural Insights into the Conformational Diversity of ClpP from Bacillus subtilis. Molecules and Cells, 2011, 32, 589-596.	2.6	49
76	Single Cystathionine β-Synthase Domain–Containing Proteins Modulate Development by Regulating the Thioredoxin System in <i>Arabidopsis</i> Â Â. Plant Cell, 2011, 23, 3577-3594.	6.6	92
77	Crystal structure of PRY‧PRY domain of human TRIM72. Proteins: Structure, Function and Bioinformatics, 2010, 78, 790-795.	2.6	37
78	Dab1 binds to Fe65 and diminishes the effect of Fe65 or LRP1 on APP processing. Journal of Cellular Biochemistry, 2010, 111, 508-519.	2.6	16
79	Structures of ClpP in complex with acyldepsipeptide antibiotics reveal its activation mechanism. Nature Structural and Molecular Biology, 2010, 17, 471-478.	8.2	194
80	Structural basis for the recognition of N-end rule substrates by the UBR box of ubiquitin ligases. Nature Structural and Molecular Biology, 2010, 17, 1175-1181.	8.2	128
81	Expression, purification and biochemical characterization of the N-terminal regions of human TIG3 and HRASLS3 proteins. Protein Expression and Purification, 2010, 71, 103-107.	1.3	17
82	Identification of a novel ubiquitin binding site of STAM1 VHS domain by NMR spectroscopy. FEBS Letters, 2009, 583, 287-292.	2.8	22
83	A simple technique to convert sitting-drop vapor diffusion into hanging-drop vapor diffusion by solidifying the reservoir solution with agarose. Journal of Applied Crystallography, 2009, 42, 975-976.	4.5	10
84	Biochemical and structural characterization of 5′-methylthioadenosine nucleosidases from Arabidopsis thaliana. Biochemical and Biophysical Research Communications, 2009, 381, 619-624.	2.1	6
85	A degradation signal recognition in prokaryotes. Journal of Synchrotron Radiation, 2008, 15, 246-249.	2.4	6
86	Purification, crystallization and preliminary X-ray diffraction analysis of a cystathionine β-synthase domain-containing protein, CDCP2, fromArabidopsis thaliana. Acta Crystallographica Section F: Structural Biology Communications, 2008, 64, 825-827.	0.7	4
87	Real-time imaging of NF-AT nucleocytoplasmic shuttling with a photoswitchable fluorescence protein in live cells. Biochimica Et Biophysica Acta - General Subjects, 2008, 1780, 1403-1407.	2.4	8
88	A Role for a Menthone Reductase in Resistance against Microbial Pathogens in Plants Â. Plant Physiology, 2008, 148, 383-401.	4.8	97
89	The recombination-associated protein RdgC adopts a novel toroidal architecture for DNA binding. Nucleic Acids Research, 2007, 35, 2671-2681.	14.5	7
90	Structural characterization of the photoswitchable fluorescent protein Dronpa-C62S. Biochemical and Biophysical Research Communications, 2007, 354, 962-967.	2.1	26

#	Article	IF	CITATIONS
91	Structural Basis of SspB-tail Recognition by the Zinc Binding Domain of ClpX. Journal of Molecular Biology, 2007, 367, 514-526.	4.2	43
92	Structural and Functional Insights into Dom34, a Key Component of No-Go mRNA Decay. Molecular Cell, 2007, 27, 938-950.	9.7	84
93	Tumoral acidic extracellular pH targeting of pH-responsive MPEG-poly(β-amino ester) block copolymer micelles for cancer therapy. Journal of Controlled Release, 2007, 123, 109-115.	9.9	281
94	STAM–AMSH interaction facilitates the deubiquitination activity in the C-terminal AMSH. Biochemical and Biophysical Research Communications, 2006, 351, 612-618.	2.1	25
95	S2c1-1 Structure and Ribonuclease Activity of Pelota : Implications for the No-go Decay and Translation Regulation(S2-c1: "Crystallographic approach to understand biological) Tj ETQq1 1 0.784314 rgBT /C Seibutsu Butsuri. 2006. 46. S120.	verlock 10 0.1	D Tf 50 582 T
96	Crystal structure of 5′-methylthioadenosine nucleosidase from Arabidopsis thaliana at 1.5-Ã resolution. Proteins: Structure, Function and Bioinformatics, 2006, 65, 519-523.	2.6	11
97	Crystal Structure of the FERM Domain of Focal Adhesion Kinase. Journal of Biological Chemistry, 2006, 281, 252-259.	3.4	108
98	Characterization of the HslU chaperone affinity for HslV protease. Protein Science, 2005, 14, 1357-1362.	7.6	16
99	Ring-shaped architecture of RecR: implications for its role in homologous recombinational DNA repair. EMBO Journal, 2004, 23, 2029-2038.	7.8	105
100	Crystal Structure of the Bowman–Birk Inhibitor from Barley Seeds in Ternary Complex with Porcine Trypsin. Journal of Molecular Biology, 2004, 343, 173-186.	4.2	29
101	Origins of Peptide Selectivity and Phosphoinositide Binding Revealed by Structures of Disabled-1 PTB Domain Complexes. Structure, 2003, 11, 569-579.	3.3	117
102	SAP couples Fyn to SLAM immune receptors. Nature Cell Biology, 2003, 5, 155-160.	10.3	259
103	Homotetrameric Structure of the SNAP-23 N-terminal Coiled-coil Domain. Journal of Biological Chemistry, 2003, 278, 13462-13467.	3.4	17
104	Structural Basis of Degradation Signal Recognition by SspB, a Specificity-Enhancing Factor for the ClpXP Proteolytic Machine. Molecular Cell, 2003, 12, 75-86.	9.7	56
105	Proteomics-based Target Identification. Journal of Biological Chemistry, 2003, 278, 52964-52971.	3.4	132
106	Functional interactions of HslV (ClpQ) with the ATPase HslU (ClpY). Proceedings of the National Academy of Sciences of the United States of America, 2002, 99, 7396-7401.	7.1	65
107	Isolation and characterization of the prokaryotic proteasome homolog HslVU (ClpQY) from Thermotoga maritima and the crystal structure of HslV. Biophysical Chemistry, 2002, 100, 437-452.	2.8	24
108	Crystal structure of human nucleoside diphosphate kinase A, a metastasis suppressor. Proteins: Structure, Function and Bioinformatics, 2002, 46, 340-342.	2.6	27

#	Article	IF	CITATIONS
109	Structural basis of non-specific lipid binding in maize lipid-transfer protein complexes revealed by high-resolution X-ray crystallography1 1Edited by D. Rees. Journal of Molecular Biology, 2001, 308, 263-278.	4.2	175
110	The Quaternary Arrangement of HslU and HslV in a Cocrystal: A Response to Wang, Yale. Journal of Structural Biology, 2001, 135, 281-293.	2.8	13
111	Crystal Structure of Klebsiella aerogenesUreE, a Nickel-binding Metallochaperone for Urease Activation. Journal of Biological Chemistry, 2001, 276, 49359-49364.	3.4	86
112	Crystallization and preliminary X-ray crystallographic analysis of human nucleoside diphosphate kinase A. Acta Crystallographica Section D: Biological Crystallography, 2000, 56, 504-505.	2.5	6
113	Crystallization and preliminary X-ray diffraction analysis ofSaccharomyces cerevisiaeYgr203p, a homologue of Acr2 arsenate reductase. Acta Crystallographica Section D: Biological Crystallography, 2000, 56, 778-780.	2.5	3
114	Crystallization and preliminary X-ray crystallographic analysis ofEscherichia coliCyaY, a structural homologue of human frataxin. Acta Crystallographica Section D: Biological Crystallography, 2000, 56, 920-921.	2.5	8
115	Nucleoside diphosphate kinase from the hyperthermophilic archaeonMethanococcus jannaschii: overexpression, crystallization and preliminary X-ray crystallographic analysis. Acta Crystallographica Section D: Biological Crystallography, 2000, 56, 1485-1487.	2.5	3
116	The structures of HslU and the ATP-dependent protease HslU–HslV. Nature, 2000, 403, 800-805.	27.8	406
117	Docking of components in a bacterial complex. Nature, 2000, 408, 667-668.	27.8	40
118	Docking of components in a bacterial complex. Nature, 2000, 408, 668-668.	27.8	5
119	Crystal structure of NAD+-dependent DNA ligase: modular architecture and functional implications. EMBO Journal, 2000, 19, 1119-1129.	7.8	169
120	Crystal structure of Escherichia coli CyaY protein reveals a previously unidentified fold for the evolutionarily conserved frataxin family. Proceedings of the National Academy of Sciences of the United States of America, 2000, 97, 8932-8937.	7.1	119
121	Mutational studies on HslU and its docking mode with HslV. Proceedings of the National Academy of Sciences of the United States of America, 2000, 97, 14103-14108.	7.1	136
122	A thermostable xylose isomerase fromThermus caldophilus: biochemical characterization, crystallization and preliminary X-ray analysis. Acta Crystallographica Section D: Biological Crystallography, 1999, 55, 294-296.	2.5	5
123	Crystallization and preliminary X-ray crystallographic analysis of deoxycytidylate hydroxymethylase from bacteriophage T4. Acta Crystallographica Section D: Biological Crystallography, 1999, 55, 1061-1063.	2.5	1
124	Crystallization and preliminary X-ray crystallographic analysis of the protease inhibitor ecotin in complex with chymotrypsin. Acta Crystallographica Section D: Biological Crystallography, 1999, 55, 1091-1092.	2.5	1
125	Crystallization and preliminary X-ray analysis of Saccharomyces cerevisiae Ypd1p, a key intermediate in phosphorelay signal transduction. Acta Crystallographica Section D: Biological Crystallography, 1999, 55, 1219-1221.	2.5	2
126	Crystallization and preliminary X-ray analysis of a complex between the Bowman–Birk trypsin inhibitor from barley and porcine pancreatic trypsin. Acta Crystallographica Section D: Biological Crystallography, 1999, 55, 1244-1246.	2.5	1

#	Article	IF	CITATIONS
127	Crystal structure of deoxycytidylate hydroxymethylase from bacteriophage T4, a component of the deoxyribonucleoside triphosphate-synthesizing complex. EMBO Journal, 1999, 18, 1104-1113.	7.8	31
128	Insights into eukaryotic multistep phosphorelay signal transduction revealed by the crystal structure of Ypd1p from Saccharomyces cerevisiae 1 1Edited by I. A. Wilson. Journal of Molecular Biology, 1999, 293, 753-761.	4.2	51
129	Crystal structure of a 16 kda double-headed bowman-birk trypsin inhibitor from barley seeds at 1.9 Ã resolution 1 1Edited by R. Huber. Journal of Molecular Biology, 1999, 293, 1133-1144.	4.2	57
130	Preliminary X-ray crystallographic analysis of Bowman–Birk trypsin inhibitor from barley seeds. Acta Crystallographica Section D: Biological Crystallography, 1998, 54, 441-443.	2.5	3
131	Kunitz-type soybean trypsin inhibitor revisited: refined structure of its complex with porcine trypsin reveals an insight into the interaction between a homologous inhibitor from Erythrina caffra and tissue-type plasminogen activator 1 1Edited by R. Huber. Journal of Molecular Biology, 1998, 275, 347-363.	4.2	230
132	The crystal structure of a triacylglycerol lipase from Pseudomonas cepacia reveals a highly open conformation in the absence of a bound inhibitor. Structure, 1997, 5, 173-185.	3.3	301
133	Crystal structure of carboxylesterase from Pseudomonas fluorescens, an α/β hydrolase with broad substrate specificity. Structure, 1997, 5, 1571-1584.	3.3	109
134	Crystal structure of Bacillus licheniformis α-Amylase at 1.7resolution. Progress in Biotechnology, 1996, 12, 163-170.	0.2	1
135	Refined Structure of the Chitinase from Barley Seeds at 2.0 Ã Resolution. Acta Crystallographica Section D: Biological Crystallography, 1996, 52, 289-298.	2.5	28
136	Crystal structure analyses of uncomplexed ecotin in two crystal forms: Implications for its function and stability. Protein Science, 1996, 5, 2236-2247.	7.6	29
137	Crystallization and preliminary X-ray crystallographic analysis of DNA polymerase fromThermus aquaticus. Acta Crystallographica Section D: Biological Crystallography, 1995, 51, 1086-1088.	2.5	1
138	Crystallization, molecular replacement solution, and refinement of tetrameric β-amylase from sweet potato. Proteins: Structure, Function and Bioinformatics, 1995, 21, 105-117.	2.6	55
139	Crystal structure of an uncleaved \hat{l}_{\pm} 1 -antitrypsin reveals the conformation of its inhibitory reactive loop. FEBS Letters, 1995, 377, 150-154.	2.8	48
140	Crystallization and preliminary X-ray crystallographic study of ribosome-inactivating protein from barley seeds. Acta Crystallographica Section D: Biological Crystallography, 1994, 50, 910-912.	2.5	1
141	Crystallization and preliminary X-ray crystallographic analysis of chitinase from barley seeds. Proteins: Structure, Function and Bioinformatics, 1993, 17, 107-109.	2.6	5